Spent Bleaching Earth Supported CeFeO₃ Perovskite for Visible Light Photocatalytic Oxidation of Methylene Blue

Check for updates

Edy Saputra[1],*, Panca Setia Utama[1], Irdoni[1], Marihot Danield Vyendri Simatupang[1],
Barata Aditya Prawiranegara[2], Hussein Rasool Abid[3,4], Oki Muraza[5]

[1]Department of Chemical Engineering, Riau University, Pekanbaru 28293, Indonesia
[2]Department of Chemistry, Faculty of Mathematics and Natural Sciences Universitas Riau, Pekanbaru 28293, Indonesia
[3]School of Engineering, Edith Cowan University, Joondalup, WA, Australia
[4]Chemical Engineering, WA School of Mines: Minerals, Energy and Chemical Engineering, Curtin University, Australia
[5]Center of Excellence in the Department of Nanotechnology and Chemical Engineering, King Fahd University of Petroleum and Minerals, Dhahran, 31261, Saudi Arabia

ABSTRACT: Dyes substances from the textile industry wastewater are internationally classified as poisonous substances, and they cause a severe threat to humans being and other living things, even at low concentrations. Therefore, this waste has to be treated before discharge to the environment. One of the most effective processes for degrading dyes is photocatalytic oxidation. Two different pretreatments of Spent bleaching earth (SBE) from palm oil refinery plant were applied to produce catalyst supports. The SBEe support was prepared by extraction using n-hexane, SBEc by calcination at 500 ℃, and then used as a support for CeFeO₃/SBEe and CeFeO₃/SBEc perovskite catalyst. Both catalysts were tested for the degradation of methylene blue (MB) using photocatalytic oxidation. The properties of catalysts were characterized using some characterization methods, such as thermogravimetric-differential thermal analysis (TG-DTA), X-ray diffraction (XRD), scanning electron microscope (SEM) equipped with Dispersive Energy X-ray Spectroscopy (EDS), specific surface area (BET) and pore size analysis. CeFeO₃/SBEe catalyst was found more efficient in photocatalytic oxidation for MB compared with the CeFeO₃/SBEc catalyst. CeFeO₃/SBEe catalyst could degrade 99.5% of MB during 120 min, at the condition of 25 mg/L MB, 1.0 g/L catalyst, and pH 7. The effect of pH on the performance of the catalyst followed the order of pH 7 > pH 9 > pH 5. Moreover, the CeFeO₃/SBEe catalyst demonstrated excellent activity in the degradation of MB, displaying that CeFeO₃/SBEe is a favorable catalyst for water purification.

Key words: Perovskite, dyes, water purification, cerium orthoferrite, environment

1. INTRODUCTION

Nowadays, the treatment of wastewater as a source of clean water is vital for society's lives, both from an economic and environmental perspective. Thus, making the development of the wastewater treatment process develop rapidly. One of the most effective methods today is the advanced oxidation process (AOP) [1]. The AOP process relies heavily on the production of highly reactive radical species such as hydroxyl radicals (OH$^\bullet$) which have high oxidation potential for the degradation of organic compounds selectively [2]. One process that is relatively attractive for researchers to study is photocatalytic for removing methylene blue (MB) from aqueous solution become less toxic substances, CO_2 and H_2O [3-5].

The solid waste generated in vegetable oil processing, such as spent bleaching earth (SBE), has properties and structures similar to zeolites, which has the main elements of Al_2O_3 and SiO_2 [6]. The bleaching earth is widely used to purify crude oil from undesirable color and impurities [7]. SBE contains more than 20% of oil by weight; it considers hazardous substances and dangerous pollutants to the environment [8, 9]. Disposing of SBE without proper handling is harmful to the environment due to the degradation of residual oil in SBE and associated with emissions of greenhouse gases in its dumping. The nature of SBE, which has a size of nano/micropores and also zeolite like composition. Therefore, SBE has potential usage after the reactivation process, such as adsorbents, filler, and support catalysis [10].

Over the past decade, the development of semiconductor catalysts for the process of photocatalysis has been increased in wastewater treatment technology. One catalyst that often used is TiO_2 because this catalyst has several advantages, such as inertness, non-toxic, and high chemical stability. However, TiO_2 also has a severe weakness, such as a high energy bandgap (3.0-3.2 eV), thus requiring UV radiation and inhibiting the effectiveness of TiO_2 [11, 12]. This deficiency is overcome by modifying the structure and chemical composition of semiconductor material by emerging new favorable properties. One of the
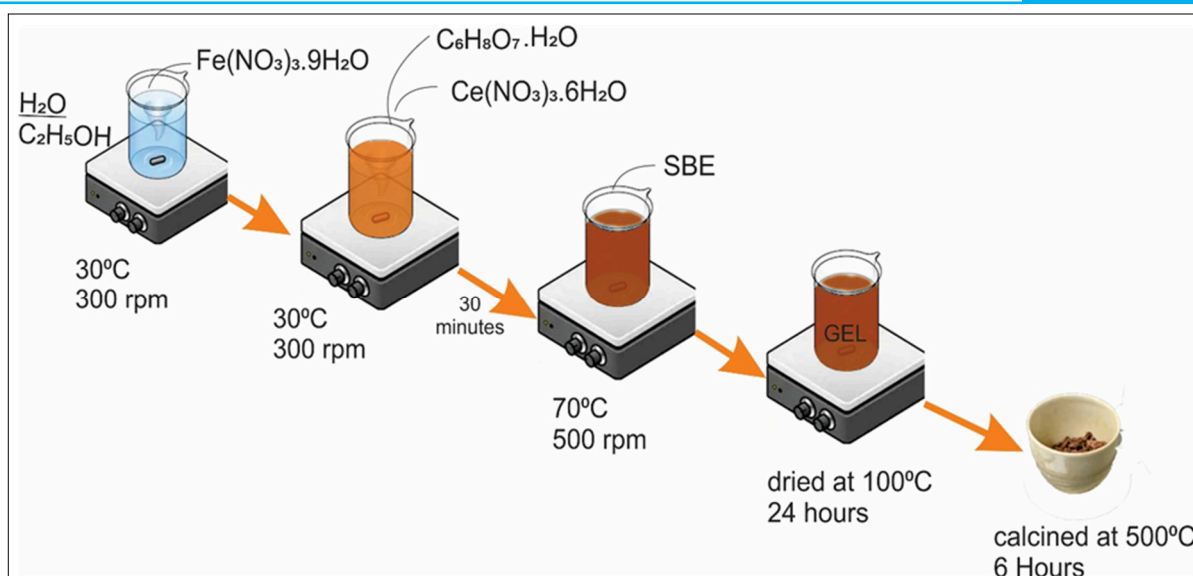
Fig. 1. Schematic of the preparation of CeFeO$_3$/SBEe and CeFeO$_3$/SBEc perovskite catalyst.

impressive materials that have been widely examined is perovskite. Perovskite, with the general AMO$_3$ formula, has cations A and/or M, which can be exchanged with foreign cations without changing their structure, but changing the oxidation status of the M cation and enter a new oxygen vacancy [13-15]. CeFeO$_3$, which is a ferrite spinel nanoparticle material with a narrow bandgap (<1.9 eV), is suitable for photocatalysts. Besides, the stable, non-toxic and magnetic nature of CeFeO$_3$ makes it easy to separate, making CeFeO$_3$ suitable for use in wastewater treatment [16, 17]

In this paper, we reported the application of low cost and eco-friendly novel semiconductor catalyst support from SBE, the waste of palm oil industry, for synthesizing CeFeO$_3$/SBEe and CeFeO$_3$/SBEc perovskite catalysts. The photocatalytic performances of both catalysts were compared under visible irradiation. Their physico-chemical properties were also characterized. Furthermore, some critical parameter such as initial pH and the concentration of MB solution was carefully considered in this study. The application of this supports in perovskite catalysts shows excellent performance in degrading MB from wastewater and has a great potential to develop further to be applied in the chemical industry.

2. EXPERIMENTAL SECTION

2.1 SBE Support

SBE sample was obtained from a crude palm oil refinery plant in Riau Indonesia, which has contained ~ 20 % of oil. Before using it as a catalyst supports, two types of SBE were pretreated with two methods, namely solvents extracted and calcined. One SBE sample was extracted by hexane and collected from suspension by filtration, then desiccated in an oven at 120°C for 24 h and represented as SBEe. The other support was attained by calcined at 500 °C for three h and denoted as SBEc.

2.2 Preparation of CeFeO$_3$/SBE composite catalyst

The preparation of the CeFeO$_3$/SBEe perovskite catalyst was prepared using a modified method (18). The reactant precursors of the compound are 2.10 g of

C$_6$H$_8$O$_7$.H$_2$O (Merck), 2.02 g of Fe(NO$_3$)$_3$.9H$_2$O (Merck), and 2.20 g of Ce(NO$_3$)$_3$.6H$_2$O (Sigma Aldrich), while the solvent is 30 mL of mixed H$_2$O/C$_2$H$_5$OH with the ratio of 1:2. Furthermore, the solution was stirred homogeneously at room temperature for 30 min. Subsequently, 2 g SBEe were added and stirred at 70°C until the gel was formed. Next, the gel dried at 100°C for 24 hours and calcined at 500°C for 6 h in air. Then the catalyst was put in storage in a desiccator while waiting for usage. The same procedure was also carried out for CeFeO$_3$/SBEc.

2.3 Catalyst Characterization

Two materials were characterized by X-ray diffraction (XRD) analysis using SmartLab SC-70, with Cu-Ka Radiation of λ = 1.54059Å. Accelerating Voltage and current was 40 kV and 30 mA. The scanning rate was 0.01s^{-1} and 2θ range of 10-90. The morphologies of the catalyst were observed using the field scanning electron microscope (A JEOL JSM-6300F, USA). EDS, energy-dispersive X-ray spectroscopy were also utilized to detect metal particles on supported catalysts. N$_2$ adsorption-desorption isotherm with the BET (NOVA 4200e, *Quantachrome*). A thermal gravimetric analyzer was used to collect the thermal stability of materials using a TGA/DSC1 STAR^e system-METTLER TOLEDO.

2.4 Photocatalyst process

The catalytic photodegradation has taken place in a 500 ml beaker glass, in a thermo-controlled water bath, containing 10-40 mg/L of MB solution (250 mL). After that, as much as 0.25 g/L of the catalyst was added. The solution was stirred at 400 rpm in room temperature (30°C ± 2°C) and illuminated with a *Mercury Lamp* 250 W (Phillips). The top of the reactor was located at a distance of 25 cm away from the light source. The solution was a place in darkness for 20 min to reach absorption and adsorption equilibrium. Next, the photocatalytic process started when turning on the light. Every interval time, samples were taken using a 0.45 µm syringe filter from the reactor, and then were 1 mL of suspension liquid collected. For adjusting the pH of the solution, HCl and NaOH solution of 1N was utilization. The

concentration of samples was analyzed using UV-Vis absorption Shimadzu 2600i. Analysis of chemical compositions of the collected SBE was carried out by an X-ray Fluorescence Spectroscopy (XRF, PW 2400, Philips).

3. RESULTS AND DISCUSSION

3.1. Characterization of catalysts

The composition of the collected spent bleaching earth (SBE) are listed in Table 1. As can be observed, SBE mostly consist of silica and alumina with particular iron and calcium oxide.

Table 1 Composition of SBE

Composition	SBE (wt%)
MgO	3.56
Al_2O_3	10.23
SiO2	61.51
K_2O	1.12
CaO	4.23
TiO	0.64
FeO	4.32
L.O.I	5.40
pH[a]	5.10

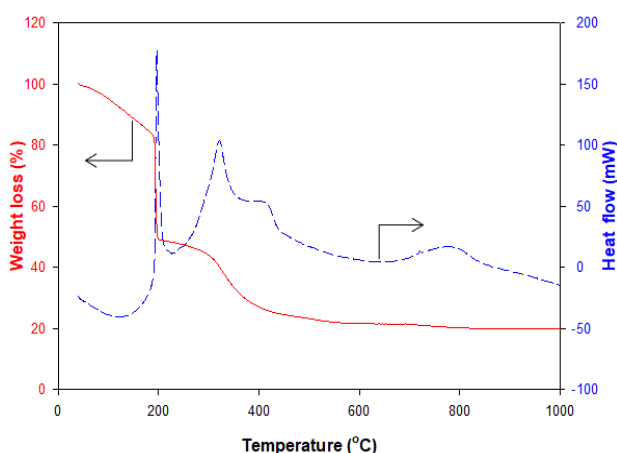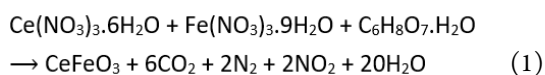[a] pH was decided by blending 0.1 g solid with 10 mL water.

Fig. 2. TGA dan DSC profiles of $CeFeO_3$/SBEe.

$CeFeO_3$/SBEe perovskite catalyst was studied by TGA and DSC under the air atmosphere (Fig. 2). The TGA patterns of catalyst show a substantial changed up to 53.5% of weight loss between 30 °C and 200 °C. It corresponds to the loss of water in the crystallization process and thermal transformation (decomposition) of organic, volatile compounds on precursor substances and a trace amount of oxygen. The exothermic peak occurred at 200 °C on the DSC curve due to the vaporization of the volatile component [18, 19]. The Following, at around 250 °C to 500 °C, weight loss of about 21.5% relates to the loss of oxygen from precursor resulting in the phase transformed into perovskite structural compounds $CeFeO_3$, as shown in the following reaction.

$$Ce(NO_3)_3.6H_2O + Fe(NO_3)_3.9H_2O + C_6H_8O_7.H_2O$$
$$\longrightarrow CeFeO_3 + 6CO_2 + 2N_2 + 2NO_2 + 20H_2O \qquad (1)$$

Three of the exothermic peaks appeared between 250 °C and 850 °C (about 320, 420, 850 °C) due to the thermal transformation of citric acid and gradual crystallization of CeFeO3. Thus, the calcination temperature of 500 °C was chosen to synthesize $CeFeO_3$ perovskite.

Fig. 3 presents the XRD spectra of supported $CeFeO_3$ perovskite catalysts, which are the utilization of two different treatments of supports. Overall, two modes of catalysts displayed a weak crystalline phase, as indicated by the observance of a relatively broad peak. $CeFeO_3$ oxide peaks are observed with diffraction peaks occurred 21.04°, 26.24°, 28,81°, 33.41°, 39.98°, 48.30°, and 57.50°, corresponding to JCPDS standard 00-022-0166 for perovskite crystalline structures. Those XRD results show a successful synthesis of $CeFeO_3$ perovskite from a sol-gel approach.

N_2 adsorption/desorption of the perovskite catalyst $CeFeO_3$/SBEe and $CeFeO_3$/SBEc, as shown in Fig. 4. While the results of the analysis of the two catalysts are shown in Table 2. The S_{BET} of the $CeFeO_3$/SBEe perovskite catalyst has a higher 20 m²/g than $CeFeO_3$/SBEc, this caused by differences in the treatment of the SBE. Moreover, both catalysts have a pore radius of less than 20 Å, indicating their microporous nature.
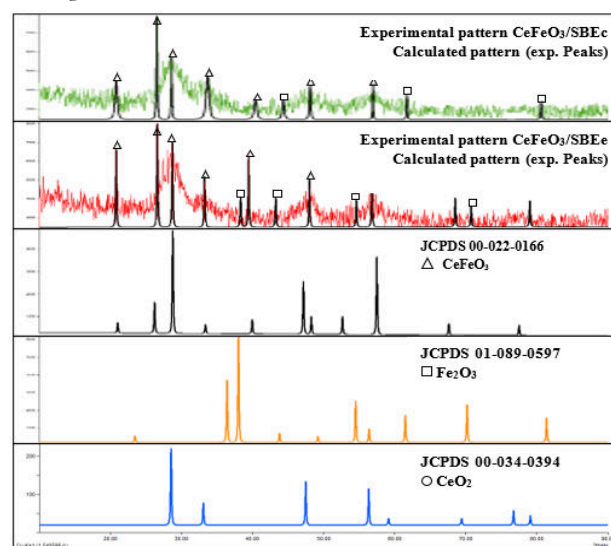

Fig. 3. XRD patterns of spent bleaching earth and their supported $CeFeO_3$/SBEe and $CeFeO_3$/SBEc perovskite catalyst.
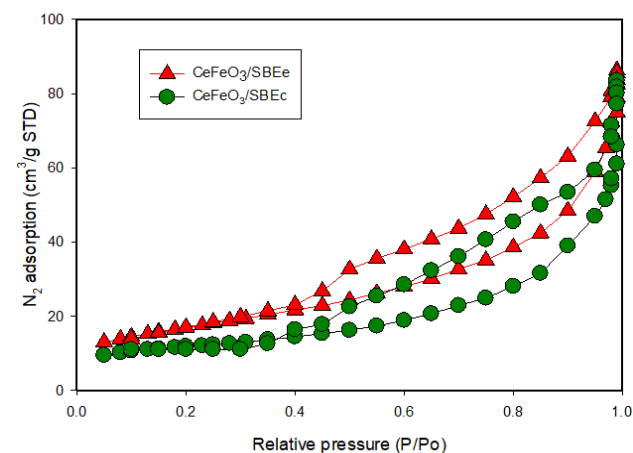

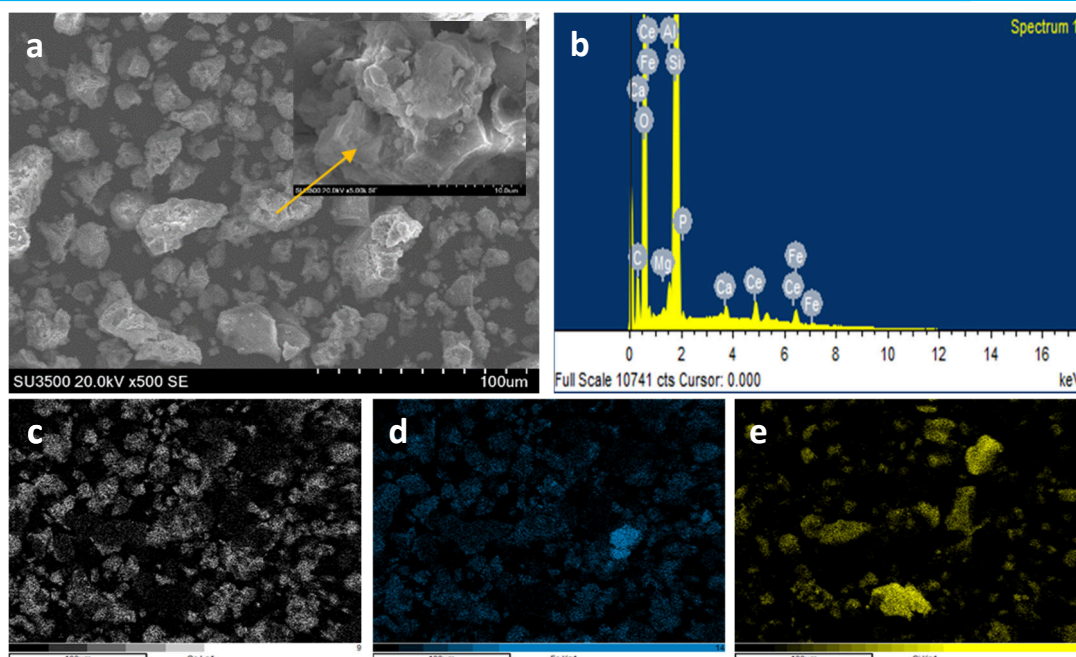**Fig. 4.** N_2 adsorption isotherm of the perovskite catalyst $CeFeO_3$/SBEe and $CeFeO_3$/SBEc.

Fig. 5. Morphologies of the CeFeO$_3$/SBEe perovskite catalyst. SEM images of samples (a), the inset demonstrates the particle magnification, (b) EDS spectrum, and (c, d, and e) the elemental mapping images.

Fig. 6. Morphologies of the CeFeO$_3$/SBEc perovskite catalyst. SEM images of samples (a), the inset demonstrates the particle magnification, (b) EDS spectrum, and (c, d, and e) the elemental mapping images.
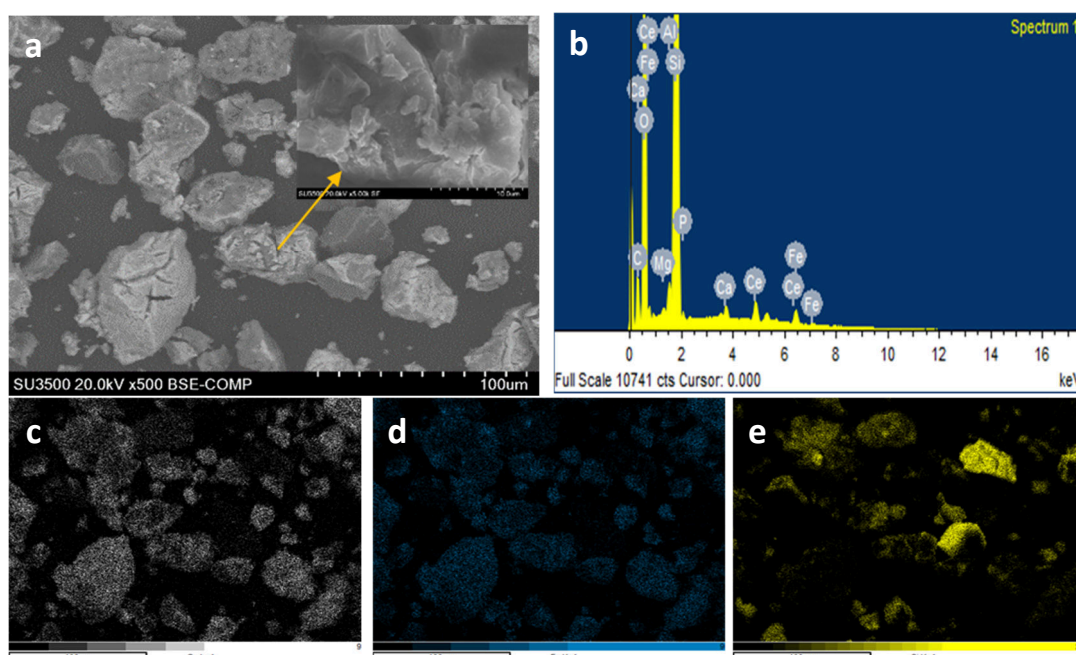
Fig. 5 and 6 present SEM images, EDS spectrum, and mapping images of supported CeFeO$_3$ catalysts. Most CeFeO$_3$/SBEe and CeFeO$_3$/SBEc perovskite catalysts exhibited agglomeration of the particles, and asymmetrical shapes with the average size of CeFeO$_3$/SBEe particles are 1-30 μm, while CeFeO$_3$/SBEc are 10-70 μm (Fig. 5a and 6a). It was apparent that the diameter of CeFeO$_3$/SBEe particles was less then CeFeO$_3$/SBEc particles. The EDS spectrum of two catalysts is shown in Fig 5b and 6b. Both samples showed the attendance of Ce, Fe, Si, Al, Ca, and Mg. Consequently, the EDS spectra implied the presence of Ce and Fe on two catalysts, conforming XRD patterns. The elemental mapping images of the particle is shown in Fig. 5c,

d, e, and Fig. 6c, d, and e, and it indicates the presence of two elements such as Ce, Fe. Both elements are equally distributed.

Table 2 BET Characterization of Catalyst

Catalyst Type	S_{BET} (m^2 g^{-1})	Pore Volume (cm^3 g^{-1})	Pore Radius (Å)
CeFeO$_3$/SBE$_e$	59.44	0.133	19.114
CeFeO$_3$/SBE$_c$	39.17	0.129	19.175

3.2. Degradation of MB by SBE supported cerium orthoferrite photocatalytic

Fig. 7 displays the photocatalytic performance of catalysts in the removal of MB under visible light irradiations. In general, there is no MB degradation in photolysis using visible light minus the presence of the catalyst. Equally, catalysts showed about 40 % MB removal in dark conditions. UV-vis light could drastically degrade MB. It shows that the efficiency of photocatalytic degradation present of the $CeFeO_3$/SBEe catalyst reached a peak of 99.5% for 120 minutes, while the $CeFeO_3$/SBEc catalyst is reached 90.68% efficiency at the same time. It shows that the efficiency of $CeFeO_3$/SBEe in photocatalytic activity is better than $CeFeO_3$/SBEc. That was attributed to several factors, such as surface area, pore size, and the particle size of the catalyst [20]. $CeFeO_3$/SBEe is demonstrated to have better efficiency than $CeFeO_3$/SBEc. This is directly related to the S_{BET} of the catalyst used where $CeFeO_3$/SBEe has a larger surface area than $CeFeO_3$/SBEc. Specifically, $CeFeO_3$/SBEe had a surface area of 59.44 m^2/g while $CeFeO_3$/SBEc had only 39.17 m^2/g. The highest surface area will give the more active sites of the catalyst. Therefore that the formation of hydroxyl free radicals ($OH^\bullet$) is more due to the electron-hole recombination process on the surface of perovskite catalyst [21]. Also, smaller particle size tends to disperse more evenly onto the solution and lead to an increase in the activity of the photocatalytic process [22]. The formation of hydroxyl free radicals will direct an oxidation-reduction reaction (redox) of long carbon chains organic compounds (aromatic) (MB, C_{16}) into smaller molecular products such as CO_2 and H_2O [23].
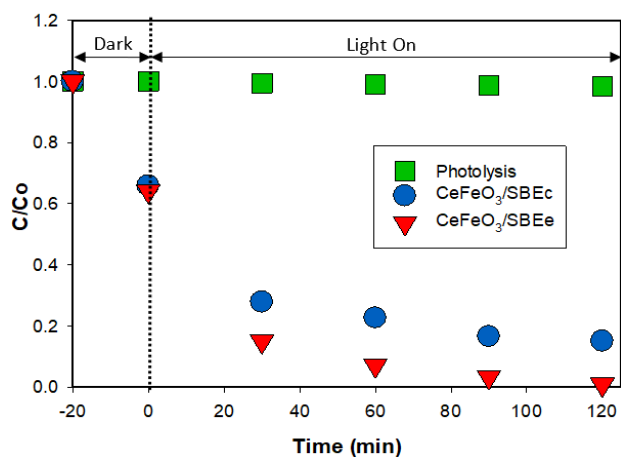

Fig. 7. MB decreased with time in photocatalytic and photolysis. Reaction condition: [MB concentration] = 10 mg/L, [Catalyst concentration] = 1.0 g/L, [pH] = 7

3.3. The effects of reaction parameters on MB degradation on $CeFeO_3$/SBEe.

Owing to the high-activity of $CeFeO_3$/SBEe, additional investigation on $CeFeO_3$/SBEe was carried out to comprehend the effect of operational conditions. The stability and activity of the catalyst under acidic, neutral, and basic conditions, were investigated under various pH conditions. The effect of pH at 5, 7, and 9 on the photocatalytic degradation is presented in Fig. 8. Overall, the pH of the Methylene Blue (MB) solution affects the photocatalytic degradation process due to the relationship between the stability of the catalyst nature and the pH solution [24]. At pH 5, MB was degraded 89.60% at 120 min, while at higher pH, which is 7.0 and 9.0, removal would be achieved at 99.5 and 94.45% in 120 min, respectively. Under acidic conditions, $OH^\bullet$ radical ions produced by the catalysis process will react with H^+ to produce H_2O compounds, and reduce the efficiency of degradation. Under higher pH conditions, OH^- ion might be more available to be converted to $OH^\bullet$ radicals. Thus, it will increase the efficiency of MB decolorization. However, at high pH value, H_2O_2 produced from the water catalyzed process would be unstable and could be decomposed into H_2O and O_2 compounds, which cannot perform degradation activities [25-27]. This phenomenon can be seen at pH 9.0; there is a slight decrease in degradation activity compared at pH 7.0. Thus, the efficiency of BM removal toward the effect of pH followed the order of pH 7 > pH 9 > pH 5. The $CeFeO_3$/SBEe perovskite catalyst has high activity at the pH range of 7-9. So, the catalyst that has been synthesized has good activity properties under various pH conditions [28].
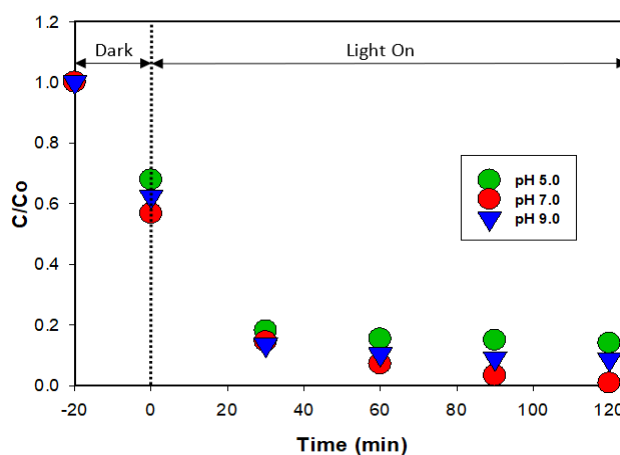

Fig. 8. Effect of pH on the photocatalytic degradation of MB. Reaction condition: [MB concentration] = 10 mg/L, [$CeFeO_3$/SBEe catalyst concentration] = 1.0 g/L
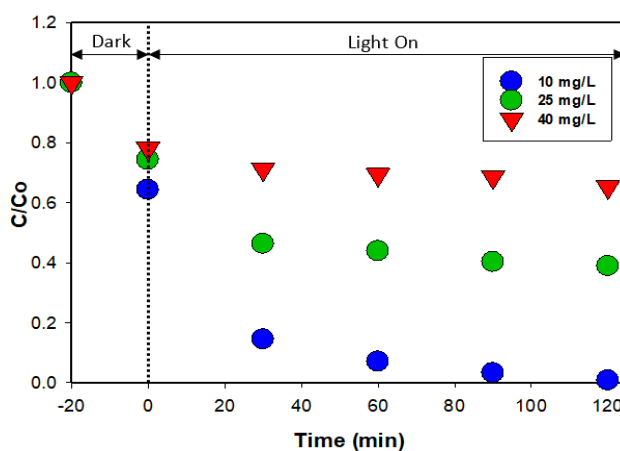

Fig. 9. Effect of MB concentration on the photocatalytic degradation of MB. Reaction condition: [$CeFeO_3$/SBEe catalyst concentration] = 1.0 g/L, [pH] = 7

The effect of initial MB concentration at 10, 25, and 40 mg/L on MB removal is presented in Fig. 9. In broad terms, the MB efficiency of degradation reduced with increasing MB concentration. At a high MB concentration, it means that more number molecules of MB are adsorbed on the surface of the CeFeO$_3$/SBEe, and the necessity of reactive species such as OH$^\bullet$ for the degradation of MB also in creases, meanwhile the amount of catalyst remains constant [29]. Moreover, increasing the initial concentration of MB will inhibit the intensity of the light that will be absorbed by the catalyst [30]. Because the amount of catalyst used is the same, the rate of formation of hydroxyl radicals (OH$^\bullet$) at each concentration of methylene blue is also estimated to be the same. So it will require more time to reach the same degradation rate, therefore reducing MB deterioration in the efficiency [17].

4. CONCLUSIONS

Spent bleaching earth (SBE) was inactive for photocatalytic degradation of MB. However, it could be used as effective support for the CeFeO$_3$ perovskite catalyst. CeFeO$_3$/SBEe perovskite catalyst demonstrated a high activity of MB removal in a visible light photocatalytic oxidation. CeFeO$_3$ was found to be presented on the catalyst, and the dispersion was higher on treated SBE. CeFeO$_3$/SBEe produced a higher efficiency in MB removal than CeFeO$_3$/SBEc. The efficiency of MB removal toward the effect of pH followed the order of pH 7 > pH 9 > pH 5. The CeFeO$_3$/SBEe catalyst can be chosen as a catalyst that is valuable for industrial applications for water purification.

■ AUTHOR INFORMATION

Corresponding Author
*Email: edysaputra@unri.ac.id

ORCID
Edy Saputra : 0000-0001-6430-9072
Oki Muraza : 0000-0002-8348-8085

■ ACKNOWLEDGEMENTS

■ REFERENCES

[1] Saputra E, Zhang H, Liu Q, Sun H, Wang S. Egg-shaped core/shell α-Mn2O3@ α-MnO2 as heterogeneous catalysts for decomposition of phenolics in aqueous solutions. Chemosphere. 2016;159:351-8.

[2] Xu X, Zhong Y, Shao Z. Double perovskites in catalysis, electrocatalysis, and photo (electro) catalysis. Trends in Chemistry. 2019.

[3] Adeleke J, Theivasanthi T, Thiruppathi M, Swaminathan M, Akomolafe T, Alabi A. Photocatalytic degradation of methylene blue by ZnO/NiFe2O4 nanoparticles. Applied surface science. 2018;455:195-200.

[4] Trandafilović LV, Jovanović DJ, Zhang X, Ptasińska S, Dramićanin M. Enhanced photocatalytic degradation of methylene blue and methyl orange by ZnO: Eu nanoparticles. Applied Catalysis B: Environmental. 2017;203:740-52.

[5] Demircivi P, Simsek EB. Visible-light-enhanced photoactivity of perovskite-type W-doped BaTiO3 photocatalyst for photodegradation of tetracycline. Journal of Alloys and Compounds. 2019;774:795-802.

[6] Wan D, Wu L, Liu Y, Chen J, Zhao H, Xiao S. Enhanced adsorption of aqueous tetracycline hydrochloride on renewable porous clay-carbon adsorbent derived from spent bleaching earth via pyrolysis. Langmuir. 2019;35(11):3925-36.

[7] Xu L, Chen S, Song H, Liu Y, Shi C, Lu Q. Comprehensively utilization of spent bleaching clay for producing high quality bio-fuel via fast pyrolysis process. Energy. 2020;190:116371.

[8] Zhang P, Dong S, Li B, Wei X, Zhang J. Durable and fluorine-free superhydrophobic coatings from palygorskite-rich spent bleaching earth. Applied Clay Science. 2018;157:237-47.

[9] Su C, Duan L, Donat F, Anthony EJ. From waste to high value utilization of spent bleaching clay in synthesizing high-performance calcium-based sorbent for CO2 capture. Applied Energy. 2018;210:117-26.

[10] Tang J, Mu B, Zong L, Wang A. One-step synthesis of magnetic attapulgite/carbon supported NiFe-LDHs by hydrothermal process of spent bleaching earth for pollutants removal. Journal of Cleaner Production. 2018;172:673-85.

[11] Safizade B, Masoudpanah S, Hasheminiasari M, Ghasemi A. Photocatalytic activity of BiFeO 3/ZnFe 2 O 4 nanocomposites under visible light irradiation. RSC advances. 2018;8(13):6988-95.

[12] Sobahi TR, Amin M. Synthesis of ZnO/ZnFe2O4/Pt nanoparticles heterojunction photocatalysts with superior photocatalytic activity. Ceramics International. 2020;46(3):3558-64.

[13] Rusevova K, Köferstein R, Rosell M, Richnow HH, Kopinke F-D, Georgi A. LaFeO3 and BiFeO3 perovskites as nanocatalysts for contaminant degradation in heterogeneous Fenton-like reactions. Chemical Engineering Journal. 2014;239:322-31.

[14] Li Y, Li Y, Yin Y, Xia D, Ding H, Ding C, et al. Facile synthesis of highly efficient ZnO/ZnFe2O4 photocatalyst using earth-abundant sphalerite and its visible light photocatalytic activity. Applied Catalysis B: Environmental. 2018;226:324-36.

[15] Wu S, Lin Y, Yang C, Du C, Teng Q, Ma Y, et al. Enhanced activation of peroxymonosulfte by LaFeO3 perovskite supported on Al2O3 for degradation of organic pollutants. Chemosphere. 2019;237:124478.

[16] Jabbarzare S, Abdellahi M, Ghayour H, Arpanahi A, Khandan A. A study on the synthesis and magnetic properties of the cerium ferrite ceramic. Journal of Alloys and Compounds. 2017;694:800-7.

[17] Anantharaman A, Priya SH, Vinosha PA, George M. Structural, optical and photocatalytic activity of cerium titanium ferrite. Optik. 2017;143:71-83.

[18] Peng K, Fu L, Yang H, Ouyang J. Perovskite LaFeO 3/ montmorillonite nanocomposites: synthesis, interface characteristics and enhanced photocatalytic activity. Scientific reports. 2016;6(1):1-10.

[19] Saputra E, Muhammad S, Sun H, Ang H-M, Tadé MO, Wang S. Manganese oxides at different oxidation states for heterogeneous activation of peroxymonosulfate for phenol degradation in aqueous solutions. Applied Catalysis B: Environmental. 2013;142:729-35.

[20] Grabowska E. Selected perovskite oxides: characterization, preparation and photocatalytic properties-a review. Applied Catalysis B: Environmental. 2016;186:97-126.

[21] Behera A, Kandi D, Majhi SM, Martha S, Parida K. Facile synthesis of ZnFe2O4 photocatalysts for decolourization of organic dyes under solar irradiation. Beilstein journal of nanotechnology. 2018;9(1):436-46.

[22] Thirumalairajan S, Girija K, Ganesh I, Mangalaraj D, Viswanathan C, Balamurugan A, et al. Controlled synthesis of perovskite LaFeO3 microsphere composed of nanoparticles via self-assembly process and their associated photocatalytic activity. Chemical Engineering Journal. 2012;209:420-8.

[23] Hao R, Wang G, Jiang C, Tang H, Xu Q. In situ hydrothermal synthesis of g-C3N4/TiO2 heterojunction photocatalysts with high specific surface area for Rhodamine B degradation. Applied Surface Science. 2017;411:400-10.

[24] Wang Q, Tian S, Ning P. Degradation mechanism of methylene blue in a heterogeneous Fenton-like reaction catalyzed by ferrocene. Industrial & Engineering Chemistry Research. 2014;53(2):643-9.

[25] Gade R, Ahemed J, Yanapu KL, Abate SY, Tao Y-T, Pola S. Photodegradation of organic dyes and industrial wastewater in the presence of layer-type perovskite materials under visible light irradiation. Journal of environmental chemical engineering. 2018;6(4):4504-13.

[26] Singh H, Rajput JK. Novel perovskite nanocatalyst (BiFeO 3) for the photodegradation of rhodamine B/ tartrazine and swift reduction of nitro compounds. Journal of the Iranian Chemical Society. 2019;16 (11):2409-32.

[27] Eskandari N, Nabiyouni G, Masoumi S, Ghanbari D. Preparation of a new magnetic and photo-catalyst CoFe2O4–SrTiO3 perovskite nanocomposite for photo-degradation of toxic dyes under short time visible irradiation. Composites Part B: Engineering. 2019;176:107343.

[28] Orak C, Atalay S, Ersöz G. Photocatalytic and photo-Fenton-like degradation of methylparaben on monolith-supported perovskite-type catalysts. Separation Science and Technology. 2017;52(7):1310 -20.

[29] Chen C-Y, Cheng M-C, Chen A-H. Photocatalytic decolorization of remazol black 5 and remazol brilliant orange 3R by mesoporous TiO2. Journal of environmental management. 2012;102:125-33.

[30] Nezamzadeh-Ejhieh A, Moazzeni N. Sunlight photodecolorization of a mixture of Methyl Orange and Bromocresol Green by CuS incorporated in a clinoptilolite zeolite as a heterogeneous catalyst. Journal of Industrial and Engineering Chemistry. 2013;19(5):1433-42.